

Gamma Ray Imaging of Small Animals Using Position-Sensitive Photomultiplier Tubes

A thesis submitted in partial fulfillment of the requirements for the degree of Bachelor of
Science in Physics from the College of William and Mary in Virginia,

By,
Julie Cella

Williamsburg, Virginia
April 16th, 2004

Acknowledgments

I would like to thank the generous support and guidance offered by my advisor Dr. Robert Welsh of the Physics Department and Dr. Eric Bradley and Dr. Margaret Saha of the Biology Department. I would also like to thank the kind advice and assistance offered by Jianguo Qian of Applied Science and Kevin Smith (William and Mary, '03). In addition, I would like to acknowledge our collaborators at Jefferson Lab, Stan Majewski, Vladimir Popov, Mark F. Smith, Andrew G. Weisenberger, and Randy Wojcik. This research would not be possible without the support of NIH, Department of Energy, National Science Foundation, The Jeffress Trust, and in particular The HHMI Science Education Program for their support of my summer research, additional semester grants, and travel grant.

Abstract

This thesis is an interdisciplinary investigation of small animals consisting of two parts. First, a comparison of NaI(Tl) and CsI(Tl) pixilated scintillating crystals will be presented based on results of resolution tests performed using 5" diameter Hamamatsu 5800 PSPMTs. Second, application of the gamma ray detectors will be assessed using a biological model. The biological model chosen to analyze is the efficacy of potassium iodide as a blocking agent to the uptake of radioiodine by the thyroid. The blocking dose of potassium iodide is tested and the implications discussed.

Table of Contents

1. Introduction.....	5
2. SPECT Demands and Resolution Tests.....	7
2a. CsI (Tl) Crystal.....	8
2b. NaI (Tl) Crystal.....	10
2c. Conclusion of Resolution Tests.....	12
3. Thyroid Blocking with Potassium Iodide as a Biological Model...12	
3a. Reasons to Study KI blocking.....	13
3b. Summary of Previous Literature on Efficacy of KI Blocking..15	
4. KI Blocking Study.....	18
4a. Data Analysis Method I: “Background Subtract”.....	20
4b. Data Analysis Method II: “Total Body ROI”.....	24
4c. Comparison of ROI data to Liquid Scintillation data.....	26
4d. Percent of Injected Dose that the Thyroid Accumulates and Assessment.....	28
5. Conclusion.....	32
Appendix A: Table III.....	33
Appendix B: Table XI.....	35
Appendix C: Computer Proficiency Requirement.....	36
References.....	41
Bibliography.....	43

1. Introduction

This project is an interdisciplinary investigation of small animals. One goal is to study gene expression in a mouse using nuclear medicine imaging techniques. Study of the mechanisms and effects of gene expression from a molecular biology standpoint are limited by our ability to “see” into the animal. The techniques up until about ten years ago were almost always moment-in-time images that often required killing the animal in order to prepare it for imaging. The team working on this project has attempted to improve the process of small animal imaging by exploiting nuclear physics techniques. The detector design balances resolution and sensitivity demands so as to trace biologically relevant processes through the body of a mouse, *in vivo*, at the molecular level. The ability to do this allows for more comprehensive research that has both theoretical and therapeutic implications. The experimental set-up uses commercially available radioactive ^{125}I labeled antibodies, ligands, and probes in its *in vivo* study. One of the challenges in designing this system was the spatial resolution demand due to the small body of a mouse. This was overcome by employing the techniques used in particle physics detection.

The isotope of iodine chosen for this detector (^{125}I) has a half-life of 60 days and emits both gamma rays and x-rays upon nuclear decay. The ^{125}I captures an atomic electron becoming an excited state of ^{125}Te with energy of 35 keV. That state decays mostly by internal conversion (~ 92%); it transfers its energy to another atomic electron, which gets ejected. So, both the electron capture and the internal conversion result in vacancies in the inner electron shells. The vacancies are filled as electrons fall down

energy levels emitting photons. Thus, the decay of each ^{125}I nucleus results in the emission of mostly 28 keV atomic x-rays with a few 35 keV nuclear gamma rays. These photons are detected when they give up some or all of their energy to the detection material, in this case, the scintillators. Ideally, the radiation incident upon the scintillator will cause the emission of several visible photons. The scintillation photons are then detected using a light sensitive measuring device – a photomultiplier tube. The type of scintillation material chosen and the properties of the photomultiplier tube are specific to both the size of the small animal chosen and ^{125}I .

The current dual-modality system in use for imaging consists of two 5”-diameter round 3292 Hamamatsu Position Sensitive Photomultiplier Tubes (PSPMTs) and a Lixi X-Ray Machine. PSPMTs have the advantage over regular PMTs in that they can detect position, as well as energy and time of occurrence, of the incident photon. The pixilated scintillating material used preserves the position of the gamma ray because each pixel is optically isolated from the ones beside it. Therefore, the photons get channeled toward the surface of the detector. The incident photons then get converted to electrons at the photocathode where they are converted to electrons. The electrons are accelerated and the current multiplied using grids of dynodes at successively more positive voltages instead of cups or plates as in regular PMTs. A 14 x 14 paired anode array at the base of the PSPMT records the electrons leaving the final dynode. The signal then gets converted by a CAMAC analog-to-digital converter and is collected and displayed by a Mac G3 computer using the software, KMAX (Sparrow, Inc.).

Both of the 3292 PSPMTs in use are mounted in a rotating gantry (Figure I), which allows one to image from any angle for planar imaging and to perform SPECT

imaging on the small animals. SPECT requires acquisition of planar images from many angles around the mouse and then software is used to reconstruct 3-dimensional slices of the animal.

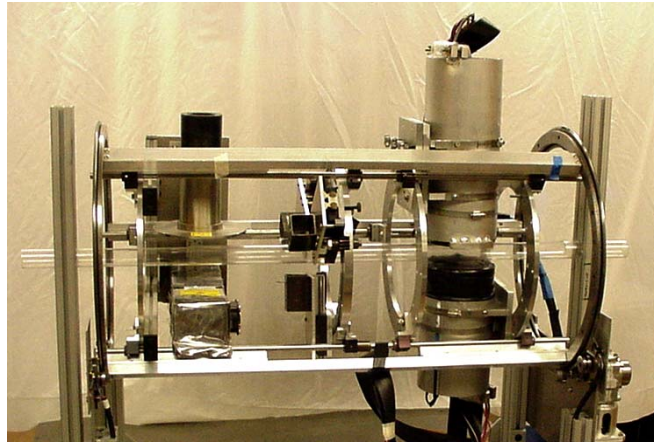


Figure I: Picture of our current set-up. Lixi X-Ray machine on left; two 5" diameter PSPMTs on right.

2. SPECT Demands and Resolution Tests

One goal of this work was to improve our SPECT capabilities. Two 2" x 2" square H8500 PSPMTs which we will be paired to create a 2" x 4" detector which is roughly the size of the mice to be imaged. Thus, whereas one was limited by geometrical constraints as to how close the detector could get to the animal during SPECT runs, it will now be possible to place the detector closer into the animal and potentially be able to perform more rapid SPECT tests. However, because the PSPMTs are adjoined there will be a region of dead space where the detectors adjoin (Figure II). This region of dead space prompts one to determine if there is a way to bridge the gap with optical coupling material to spread the light without losing overall resolution. So, comparative resolution

tests were performed using the existing 3292 PSPMTs with both types of available scintillating crystals, NaI(Tl) and CsI(Tl).

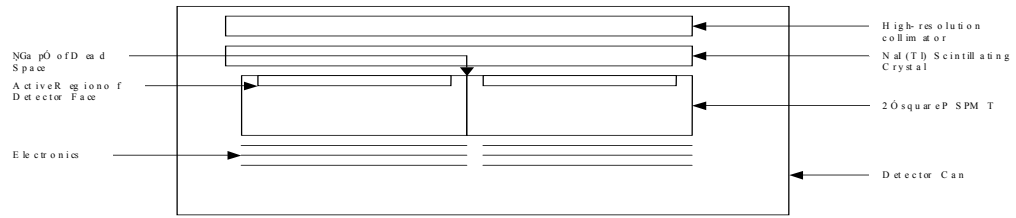


Figure II: Schematic of design of two 2" square PSPMTs butted together, viewed from the side.

2a. CsI (Tl) Crystal

The investigation was initiated with a 1" square CsI pixilated scintillating crystal with pixel size 0.35 mm x 0.35 mm x 3.0 mm size. The separation between the pixels was 0.35 mm (Figure IIIa). This crystal is intended for a 1" square PSPMT. Despite testing a range of high voltage and discriminator settings for the 3292, it was not possible to resolve the pixels and to map the crystals (Figure IIIb).

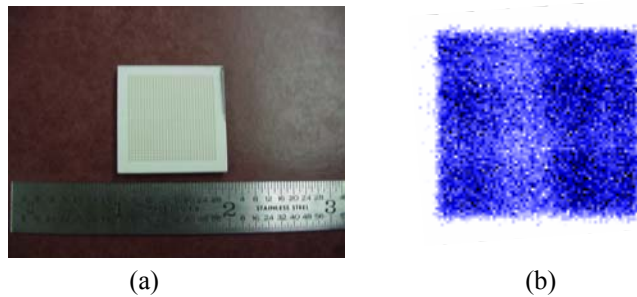


Figure III: (a) 1" CsI(Tl) crystal (b) Image raw with no resolved pixels.

We concluded that the crystal size was too small for the 3292 PSPMT. So, tests were performed on the round 5" CsI scintillating crystal that is used for our animal imaging. This crystal has a pixel size of 1 mm x 1 mm x 3 mm (Figure IV). The pixels could easily be resolved on this crystal. Resolution tests were performed using this crystal with optical grease and a piece of glass as coupling materials.

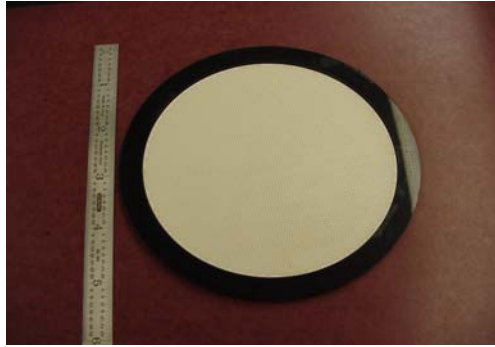


Figure IV: 5" CsI crystal with 1mm x 1mm x 3mm pixel size

The procedure for the test is as follows:

- (1) A piece of glass of thickness 1mm was placed on the surface of the detector. On top of that was placed the CsI(Tl) crystal.
- (2) Crystal mapping was run using ^{137}Cs as a source and a high voltage setting of -850V . I placed the high-energy ^{137}Cs about 6 inches from the face of the detector so that it would effectively function as a point source to the crystals of size 1 mm square. The system collected data overnight (~ 12 hours), until the pixels were easily resolved.
- (3) Next, the raw histogram from the data acquisition program was imported to the crystal-mapping program. Lines were then drawn to tell the program where the pixels were and then the program creates a crystal look-up table.
- (4) The crystal look-up was integrated into the scripts of the data acquisition program.
- (5) An 8 mm-thick high-resolution parallel hole collimator (etched Cu-Be, Tecomet) was placed on top of the crystal to prepare for the resolution tests.
- (6) Then, three 10-minute tests were run with a two-dot phantom of ^{125}I . This required a high voltage setting of -990V . The phantom was placed on the surface of the detector can.

(7) Calculations were made of the full width at half max for each trial and averaged the results.

(8) The process was repeated with no glass on the detector face.

(9) The process was repeated with a dab of optical grease on the detector face.

However, this was unsuccessful because the grease completely blurred the crystals, which made the mapping of pixels impossible (Figure V). Thus, I abandoned the optical grease as a viable coupling material.

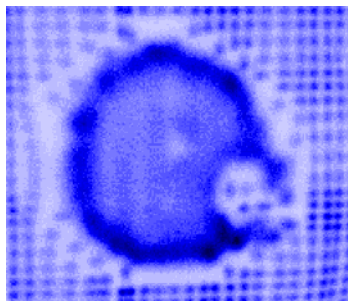


Figure V: Grease completely blurs pixels during crystal mapping; crystals not covered by grease resolve well.

The results of these tests are summarized in Table I, below:

Type of Coupling	FWHM (in)	FWHM (mm)
None	0.15 in	3.8 mm
Glass*	0.09 in	2.3 mm
Optical Grease**	NA	NA

Measured Distance between dots: 0.47 in, 1.2 mm

*Note: Thickness of glass: 1 mm, 0.04 in

**Note: The Optical Grease completely blurred the pixels.

Table I: Summary of mean FWHM for CsI Crystal with various coupling devices.

2b. NaI (Tl) Crystal

Next, the experiment was continued using a 1" NaI(Tl) pixilated crystal (manufactured by Bicron/St. Gobain). There are several key differences between the CsI

and NaI crystals. First, NaI is a hygroscopic material so the crystal must be sealed completely in glass; it rapidly deteriorates when exposed to the water vapor in air. Also, the pixels are particularly frail. While the central pixels on the crystal are 1 mm x 1 mm x 1 mm, the pixels around the edge are made to be 2 mm x 1 mm x 3 mm. Otherwise the pixels would easily crumble or fall over (Figure VI). Also, NaI(Tl) is a more efficient scintillator; it produces more photons per gamma ray. Thus, NaI has the advantage of collecting data faster.



Figure VII: 1" square NaI(Tl) Crystal. Note the wider crystal around the edge and glass that seals the crystal

The procedure is the same for NaI as listed for CsI with the following exceptions:

- (1) The high voltage setting used for the crystal mapping (^{137}Cs source): - 850V
- (2) The high voltage setting used to image the two-dot phantom (^{125}I source): -950V
- (3) Note: "No optical coupling" for NaI(Tl) actually has a layer of glass already there to seal the hygroscopic crystal. Likewise, "glass" has a double layer of glass present.

The results of these tests are summarized below in Table II:

Type of Coupling	FWHM (in)	FWHM (mm)
None*	0.14 in	3.6 mm
Glass**	0.12 in	3.0 mm
Optical Grease	0.23 in	5.8 mm
Glass** and Grease	0.19 in	4.9 mm

Measured Distance between dots: 0.47 in, 1.2 mm

*Note: There is a layer of necessary glass to keep the hygroscopic crystals from deteriorating.

**Note: Thickness of glass: 1 mm, 0.04 in

Table II: Summary of mean FWHM for NaI Crystal with various coupling devices.

2c. Conclusion of Resolution Tests

Surprisingly, we found that the resolution improved with glass in all cases. The application of optical grease completely blurred the pixels of CsI no matter what the pixel size. It degraded, though not completely, resolution for the NaI crystal. This information will be used in the design and implementation of the two new 3292 PSPMTs. We note that the 8500 PSPMTs are capable of more precise resolution. The radioactive dots of the phantom do have a finite diameter that was not taken into consideration because we only needed a comparison for the purpose of this study.

3. Thyroid Blocking with Potassium Iodide as a Biological Model

The second main component of this project was to create a means by which quantitative data could be obtained from the gamma camera images and used for detailed physiological study. To achieve this goal, we first needed to select an appropriate biological model to study. As discussed earlier, ^{125}I is the imaging isotope used in the experimental design because of the energy of its gamma-ray emission and relatively long half-life (60 days). Iodine also has biological roles in the body; it is an integral

component of hormones produced by the thyroid. Thus, the thyroid has a mechanism to transport iodide into the tissue where the iodine is then organified into hormone.

Injection of ^{125}I iodide into a euthyroid species would therefore result in the accumulation of that ^{125}I in the thyroid. Given the basic nature of iodide metabolism in the body and iodide's easy commercial availability, it seemed a logical choice for this study. We chose to examine the biodistribution of radioiodine in the body and the block of its uptake by potassium iodide. Stable potassium iodide administration is the accepted prophylaxis to block the thyroid from accumulating and organifying radioiodide.

3a. Reasons to Study KI blocking

Radioiodine accumulation by the thyroid, while a relatively simple metabolic process, is a non-trivial study in current biological research. There are several important reasons to study radioiodide accumulation by the thyroid and the efficacy of stable potassium iodide as a block to that uptake. First, there is a risk of exposure to radioisotopes in the event of a nuclear power plant accident as was seen in Poland as a result of the Chernobyl reactor accident and at Three Mile Island. Also, with the increase in nuclear medicine, the risk of radiation exposure extends to hospitals handling radioactive isotopes. Exposure to ^{137}Cs occurred at an abandoned Brazilian hospital^[1]. There is also the danger of exposure to radiation resulting from an act of terrorism.

In addition to the dangers associated with accidental exposure, there is reason to study radioiodide accumulation in the thyroid from planned procedures. Many treatments for cancer in particular now use radiation therapies that involve tagging a ligand with a radioisotope of iodine. Some iodine detaches from the ligand due to the molecule's instability and the body is exposed to more radioiodine when it metabolizes the

compound. ^{131}I is incorporated into metaiodobenzylguanidine (MIBG) and used to treat children with neuroblastoma^[2,3]. One consequence of improved survival rates among patients receiving this therapy is that side effects of the treatment, the accumulation of ^{131}I in the thyroid, must be analyzed further. Also, ^{125}I is linked to fibrinogen and administered to patients after hip surgery^[4].

Radioiodide in the body can cause health problems. The most drastic consequence is radiation-induced thyroid cancer^[1]. The correlation between radioiodide exposure and thyroid cancer has been studied^[5,6] in an attempt to determine at what dose radioiodine becomes carcinogenic. The FDA asserts exposure should not exceed 500 cGray for adults and 5 cGray for children and pregnant or lactating women^[7]. Adverse effects besides cancer include hypothyroidism, thyroiditis, and thyroid nodules and adenomas^[3]. Due to the risks incurred by exposure, every effort should be taken to determine an appropriate prophylaxis to protect the thyroid. Currently, the dose recommended is 130 mg of KI for adults and its protective effect lasts 24 hours^[7].

Aside from testing the effectiveness of the blocking dose in the event of radioiodine exposure, iodide kinetics in the body have become increasingly important in research. Since the cloning of the rat and human forms of the protein in 1996, the sodium iodide symporter (NIS) has become an important tool in research as a reporter gene in gene therapy^[8]. NIS is the transporter responsible for concentrating iodine in the tissue of the thyroid gland, the stomach, and the lactating breast. Thus, if NIS is present in a gene vector, the vector's location, efficiency in the target tissue, and proliferation or degradation can be monitored, non-invasively and in vivo, by imaging with radioiodide^[9]. Dingli proposes that the properties of NIS make it close "to being the ideal reporter

gene^[9]. Thus, our ability to image NIS in thyroid tissue responsibly would be extremely important step to imaging NIS activity in gene vectors.

For these reasons, we chose to study the efficacy of potassium iodide as a blocking agent to accumulation of radioiodide by the thyroid.

3b. Summary of Previous Literature on Efficacy of KI Blocking

Before beginning our current investigation, I performed a thorough search of current literature. Several questions guided the direction of the research. One goal was to determine different strategies for investigating how radioiodine distributed throughout the body and how results of KI block efficacy were represented. Next, I was concerned with what the results of these studies were so that this study could be compared with others. Finally, we investigated uses of gamma-ray imaging to study biodistribution in general and biodistribution of iodide in particular as a means for visualization.

There are several ways to study distribution of radioactive ligands in lab animals. One of the most common methods is to inject the isotope into the animal, allow a set amount of time post-injection to elapse, and then sacrifice the animal. After the animal is euthanized, the organs and an aliquot of blood can be excised and counted scintigraphically using a standard gamma-counting well^[10, 11, 12]. This method is effective because it ensures that one is counting the organs of interest, the blood provides a reliable method of normalization, and the efficiency of the system is easily determined by counting a stock of the isotope. However, the method involves the sacrifice of the animal and as a result requires a large number of animals and prohibits the possibility of longitudinal study.

Another method of study is urinary analysis of excreted iodide^[13, 14]. Excess iodide is either accumulated in the stomach and passed through the bowels or excreted by the kidneys as a component of urine. Thus, by knowing kidney efficiencies and counting the activity in the urine, one can determine how much iodide the animal accumulates by knowing how much is excreted. This method of investigation has no way of determining precisely where the iodide is being acquired in the body; it can only measure the clearance rate of the injected radioiodine.

There are a few other studies that use methods specifically to study uptake of radioiodine by the thyroid. Yu and Shaw developed a cuff to shield the body of the mouse only exposing the neck to a probe to count activity. They determined after 24 hours, the activity in the neck was equal to the activity in the actual thyroid (a sub-set of animals were analyzed both pre-dissection with the collar and post-dissection by counting the actual thyroid). So, at 24 hours post-injection, the activity in the neck was determined and assumed to be the activity in the thyroid^[15]. This is an effective means to study biodistribution after distributions are static. However, one aspect of our goal is the ability to study time-dependent behavior which is excluded from such a study. Also, the means of measuring the injected dose involves a different geometry than measuring the accumulation in the neck. Another strategy to determine KI block efficacy is retrospective study performed using human subjects who had undergone treatment for cancer. As discussed above, these patients are exposed to radioiodide as a result of their treatment for the cancer. This study did not try to measure the accumulation in the thyroid; rather it assessed patient health years after the treatment^[3]. Finally, a computer

simulation was developed based on a compartmentalization model of iodide in the body^[16].

While the methods of investigation varied widely, the representations of their findings fall into two main categories. Most studies represent accumulation by the thyroid as a percentage of the injected dose that they measure in the thyroid and, where applicable, on a per-gram of tissue basis^[17]. This allows for easy comparison of accumulation between treatment groups. The other method described is to determine the “protective effect” of the KI therapy. The protective effect is defined as the percent of accumulation in the thyroid eliminated by the potassium iodide block^[13, 16]. The former method is a general way to study biodistribution while the later is a more specific way to study iodide distribution relevant to blocking dose effectiveness.

A concise and useful summary of all the results is a difficult task because of the myriad of ways in which the relevant studies were conducted, results displayed, and animals used. However, Table III (Appendix A) is a representation of the results. As demonstrated in Table I, the amount of activity the thyroids of the animals/humans were exposed to varied greatly in addition to the amount of KI blocking used. No clear blocking dose is seen to be effective across the studies. What does seem to be apparent is that a plateau effect is seen in the studies done with variable blocking doses^[15, 18, 19]. There is a dose that “saturates” the thyroid against further protection by potassium iodide. Furthermore, the effectiveness of the block cannot be determined unless it is correlated to the dose of radiation that the thyroid is receiving and whether that dose is safe. In order to do this, the isotope of iodine used must be considered owing to the different energy spectra emitted by the various isotopes of iodine.

There have also been a few studies done on patients receiving treatments of radioiodine-tagged ligands. One study was a retrospective study of children who received treatment for neuroblastoma with ^{131}I -MIBG. Patients were examined an average of 2.3 years after undergoing treatment and 52.4% displayed some amount of thyroid dysfunction^[3]. Another study done on patients undergoing the same treatment noted 40% of patients suffering hypothyroidism after a follow-up at 11 months^[2]. In both studies the patients underwent a standard protocol of KI blocking which entails 100 mg of KI administered 2 days before and up to 4 weeks after surgery. These data indicate that the KI block administered to the patients is not enough to protect the thyroid. Even if the same physical amount of iodide accumulation is proven safe for ^{125}I , the higher energy of ^{131}I must be taken into consideration. Thus, blocking must be particularly effective when ^{131}I is administered to a patient. Combined with the variability in the studies outlined above this suggests that further investigation of the efficacy of KI as a blocking agent is warranted.

4. KI Blocking Study

To begin our investigation, an appropriate dose of KI to administer to the mice was established. The FDA recommends a 130 mg KI per 60 kg of body mass^[7]. This will be referred to as the “human dose.” This corresponds to a dose of ~ 2.2 mg KI per kg body mass or 2.2 μg KI per gram body mass. Thus, for the mice in this study, a “1x” animal is given 2.2 μg KI times the mass of the animal.

The KI solution was prepared by dissolving 100 mg of KI in 10 mL of water. Each “KI-group” mouse (n=3) in the first series of the study was given a 10x dose of potassium iodide by administering the appropriated aliquot of the KI solution orally one

hour before the start of imaging. This corresponds to 70 μg KI for each 30 gram mouse, or $\sim 70 \mu\text{L}$. A control group ($n=3$) was also tested. About fifteen minutes before the administration of the radioisotope, the mouse was anesthetized interperitoneally with an anesthetic, pentobarbital. As stated, one hour after the blocking dose was given, 12 μCi of ^{125}I in 100 μL of 0.9% saline was injected intramuscularly into the right femoral bicep (right leg muscle). The animals were then imaged for one hour and returned to their cages. The imaging software, KMAX, records both spatial and temporal information from the imaging period as event files. Summed five-minute time cuts of the data are then made with the data analysis package, IDL. The time cuts are then viewed and certain regions are highlighted with Region of Interest (ROI) boxes. Each ROI is then summed and analyzed and a plot is returned indicating counts per ROI versus time. The assumption that only small changes in a given ROI will occur throughout a five-minute period had previously been tested in other studies.

As discussed earlier, while it is valuable to be able to image parts of the body for diagnostic and visualization purposes; in a physiological study it is important to have quantitative data to support findings. Thus, a rigorous method of data analysis was developed and assessed. I proposed two methods to analyze the data from this study to develop a standard procedure for data analysis in similar future biological study. Furthermore, we wish to compare our findings to previous data on the effectiveness of potassium iodide as a blocking agent for uptake of radioiodide by the thyroid. In this case the objective was to elucidate the percentage of the total injected radioiodide that lodges in the thyroid after one hour of imaging.

4a. Data Analysis Method I: “Background Subtract”

The first method was to assume that the entire injected dose of radioiodide was located at the injection site at the start of imaging. This value was inferred by placing a standard 10 pixel square ROI encompassing the injection site and using the counts in that ROI from the 0 -5 minute time-cut. I assumed that amount of activity was the “total injected dose.” Next, I found the activity in the thyroid, stomach, and chest regions again using the 10 pixel square ROI for the 55 – 60 minute time-cut. Each of these values represents the activity in thyroid, stomach, and chest at one hour. The chest values were subtracted from the thyroid and stomach counts with the intent to remove “body-background” counts from the ROIs introduced by normal vascularization of areas above and below the stomach or thyroid as well as the areas around the organs. 10 x 10 ROIs are a useful standard size, but some organs of interest are somewhat smaller than such an ROI. Figure VII shows a mouse after one hour of imaging with and without ROI present for comparison. After background subtraction, the remaining activity in each ROI could be attributed to the NIS-symporter accumulating iodide in the tissue of the thyroid or the lumen of the stomach. The activity in each tissue was divided by the “total injected dose” to recover a percentage. Listed in Table IV are the counts in each ROI.

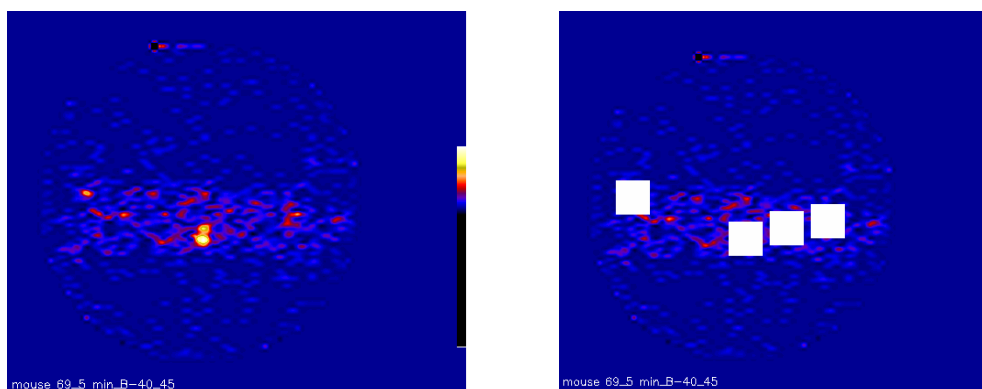


Figure VII: Image on left is mouse 69 after one hour of imaging; image on right is same mouse with ROIs diagramed

Dose	Mouse No.	Inj. Site	Stomach		Thyroid		Chest	
No KI	69	393.003	218.47	150.16	83.732	15.428	68.304	0
No KI	71	864.011	213.75	125.61	141.98	53.841	88.143	0
No KI	73	875.913	254.65	155.31	166.62	67.273	99.347	0
10x	70	218.362	231.45	170.48	58.556	-2.415	60.970	0
10x	72	846.863	301.50	222.89	104.21	25.599	78.612	0
10x	74	925.120	153.23	57.917	89.141	-6.168	95.309	0

Table IV: The ROI size was set at 10 pixels square for all analyzed ROIs. The injection site counts are taken from the 0-5 minute time cut. The counts for the other ROI's are for the 55-60 minute time cut. The first column under each ROI is total amount of counts and the second column is the data that has the body background of the mouse, taken at the chest region, subtracted out.

Table V shows the percentage of the injected activity that was in each ROI (stomach and thyroid) for a five-minute accumulation period after a total of 60 minutes of imaging.

The formula used was as follows:

$$\% \text{ of injected dose in ROI} = \frac{[\text{ROI (at 60 min)} - \text{background (at 60 min)}]}{[\text{inj. Site (at 5 min)} - \text{background (at 5 min)}]} \times 100$$

Dose	Mouse No.	% in thyroid	% in stomach
None	69	3.8%	38.2%
None	71	6.2%	14.5%
None	73	7.7%	17.7%
10x	70	NA	78.1%
10x	72	2.9%	26.3%
10x	74	NA	6.3%

Table V: Percentage of total injected dose in Stomach and Thyroid one hour after administration of ^{125}I with background subtraction.

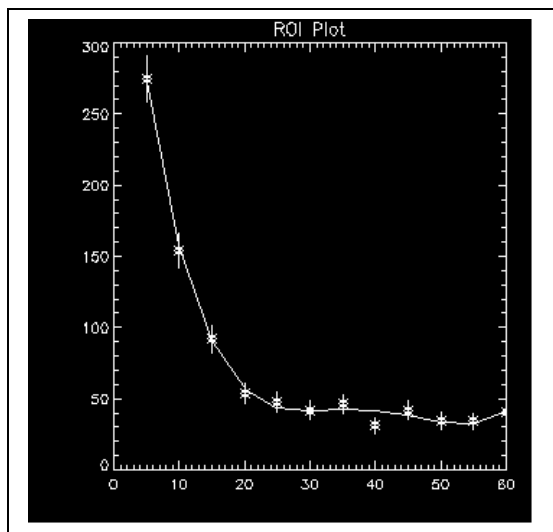
The N/A values listed above result because the background ROI had a greater amount of counts than the region of the thyroid for the given five-minute interval. This raised questions concerning the validity of this background subtraction method in general and the placement of the background ROI in particular. To test for consistency, we determined the percentage of the injected activity that was in each ROI after 60 minutes of imaging without subtracting the background out (see Table IV).

Dose	Mouse No.	% in thyroid	% in stomach
None	69	18.6%	55.6%
None	71	15.8%	24.7%
None	73	18.6%	29.1%
10x	70	21.3%	106.0%
10x	72	12%	35.6%
10x	74	9.5%	16.6%

Table VI: Percentage of total injected dose in Stomach and Thyroid one hour after administration of ^{125}I without background subtraction.

With this method, we note no discernable pattern to the data. The mice with the KI block do not show less uptake at the thyroid in either method and the higher percentages in the background subtract method do not correlate to the higher percentages found using the raw counts. Furthermore, mouse 70 has a greater amount of activity in the stomach ROI after an hour than the assumed “total injected dose.” Accordingly, this method was rejected for two reasons. First, it is not appropriate to assume the entire injected dose remains in the injection site during the first time cut. After the dose is

injected, the mouse is restrained and centered on the face of the detector. Each time-cut used here encompasses 5 minutes. The mouse metabolism is so rapid, that those few minutes cannot be ignored especially since the isotope leaves the injection site rapidly. Graph I is a sample ROI plot of the injection site ROI. This concern of time delay and “total dose” calculation suggests the second method of analysis.

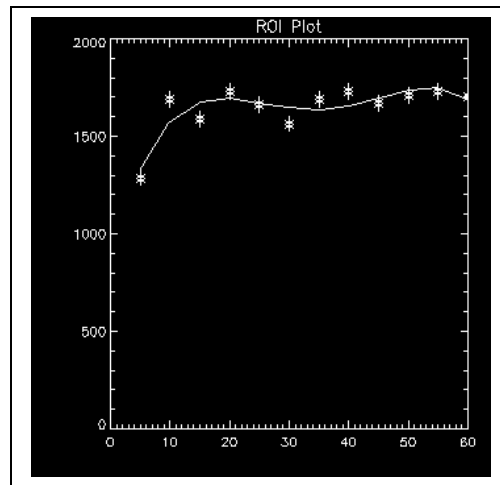


Graph I: Sample ROI plot (Mouse No. 70) showing rapid loss of activity from injection site; time (in minutes across x-axis), counts along y-axis.

Another reason the first method of analysis was rejected is the selection of “background.” The higher counts that result in the chest ROI than in the thyroid ROI, is most likely due to the extremely high vascularization of the chest cavity due to the presence of the heart and lung. So, one would not be comparing two regions of the body that have comparable physiologies with that approach. That leads to the question of determining an appropriate selection of background and how to select it. Ideally, it should be a region of the mouse body that is most similar to the neck in terms of blood flow and organ content while not being so small as to introduce random error. The question of background placement will be addressed later.

4b. Data Analysis Method II: “Total Body ROI”

This method involves using rectangular ROIs of variable sizes. ROIs to fit over the entire mouse body were constructed and analyzed. The total counts in each five-minute time cut over the course of the imaging remained constant, thus indicating that no radioiodide was leaving or entering the body (Graph II) while the biodistribution of the isotope within the body was being examined.



Graph II: Sample ROI plot showing consistency in total activity in mouse during the one hour of imaging. Plot is for mouse 72.

Thus, a reliable data point for the total injected dose was found and measured with the same modality used for all the other ROIs. Then, ROIs were placed over injection site, stomach, thyroid and nose and each was analyzed. Each ROI size was changed to fit the organ of interest in hopes of eliminating activity not attributed to the organ in the ROI. Thus, no background subtraction was used initially. The counts in each ROI at 50 – 55 time cut are recorded in Table VII.

Mouse No.	Total Body	Inj. Site	Stomach	Thyroid	Nose
69	1026.96	35.2700	168.030	24.1001	4.73310
71	1523.00	119.754	171.581	40.3121	16.8113
73	1629.27	100.870	197.637	34.6261	11.1056
70	987.963	28.2032	165.622	11.6331	8.15278
72	1732.95	196.792	222.273	25.0216	17.0644
74	1558.41	187.708	129.037	18.0126	8.81745

Table VII: Counts per ROI for Total Body ROI analysis. Note: the ROI size was varied to “fit” each organ of interest.

Again, the percentage of the total injected dose in each ROI was calculated. This time, because the variable ROI sizes were used to limit background interference from other organs and blood, background subtraction was not used in calculating these values.

Table VIII lists these results.

Dose	Mouse No.	Inj. Site/Tot.	Stomach/Tot.	Thyroid/Tot.	Nose/Tot.
None	69	3.43%	16.36%	2.35%	0.46%
None	71	7.86%	11.27%	2.65%	1.10%
None	73	6.19%	12.13%	2.13%	0.68%
10x	70	2.85%	16.76%	1.18%	0.83%
10x	72	11.36%	12.83%	1.44%	0.98%
10x	73	12.04%	8.28%	1.16%	0.57%

Table VIII: Percentage of total injected dose, obtained with total body ROI, in Stomach and Thyroid one hour after administration of ^{125}I without background subtraction.

This method reveals that the 10x blocking dose of potassium iodide limits uptake of radioiodine as postulated. The mean percentage of radioiodine in the thyroid of unblocked animals is 2.4% while the percentage in blocked animals with 10x the human dose is 1.3%. However, these numerical data are only useful for comparative purposes. We cannot conclude that the mean amount of radioiodine that goes to the thyroid in a mouse is 2.4%. We have not considered the areas above and below the stomach and thyroid, for example. Thus, this method of analysis gives a good procedure for

determining the total injected dose, but it does not eliminate the need to subtract a body background from our ROIs.

4c. Comparison of ROI data to Liquid Scintillation data

To limit the imprecision of these two methods of analysis, we sought to calibrate the system of analysis. As discussed earlier, one way to know that one is analyzing the thyroid and only the thyroid is to dissect the animal at the end of the imaging and measure the activity of ^{125}I in body parts with a standard liquid scintillation system. Another series of mice were therefore examined. This time, mice were examined at 1x (n=2), 5x (n=2), 10x (n=1), and control (n=1). The same basic procedure outlined above was followed except after the hour of imaging, the mice were euthanized and dissected according to a procedure approved by the Animal Handling and Ethics Board. The organs were then placed in liquid scintillation (LS) vials and activity was measured with a standard liquid scintillation system (Beckman Coulter, LS 6500). Those results were compared with our ROI analysis. One goal was to be able to consistently correlate the numerical data from the LS with the ROI analysis and to be able to draw firm conclusions as to an appropriate method of data analysis. With a self-consistent method for analysis, one may be able to confidently draw physiologic conclusions concerning the efficacy of potassium iodide as a blocking agent and the applicability of the PSPMT to such studies. The following series of data comparisons describe our work to determine if the data obtained from ROI analysis are consistent with the data obtained from the dissection and subsequent analysis by LS.

First, ratios of thyroid accumulation to stomach accumulation were made for each animal using both the LS and ROI data. The stomach and thyroid were selected as

organs for normalization between the two methods because the thyroid is the organ of interest in this study and the stomach is easily recognizable for ROI analysis, easily separated during dissection, and generally consistent in its uptake of iodide. The results are shown in Table IX.

Mouse No.	ROI analysis	L.S. analysis	Disparity
130	0.201	0.089	0.112
131	0.086	0.037	0.049
133	0.133	0.110	0.023
134	0.101	0.041	0.068
135	0.073	0.027	0.046
137	0.107	0.030	0.077

Table IX: Comparison of Thyroid Accumulation to Stomach Accumulation one hour after treatment with ^{125}I using ROI plots and standard Liquid Scintillation System.

As illustrated, there is some disparity between the two methods. The perceived amount of radiation in the thyroid compared to the stomach is greater for the ROI plots than in the actual dissection. This supports the rationale for background subtraction. The disparity is most likely due to inclusion of blood from around the thyroid and nearby salivary gland in the thyroid ROI. The thyroid is so small in comparison to the stomach; it is plausible to assume that background interference would be seen more intensely in the thyroid. Therefore, background was subtracted for the thyroid region using the nose ROI as a background region. Selection of the nose seemed to be more appropriate than the chest because its vascularization is more similar to the area around the thyroid. The same ratios were taken as in Table IX when accounting for the background in each ROI. For this subtraction, though, we used a “per pixel” method because the background ROI at the nose is different size from the stomach ROI. The thyroid and nose ROIs were both the same size and thus the subtraction was straight forward. We thus define:

$$[(\text{Stomach}/\text{Area}) - (\text{Nose}/\text{Area})] \times \text{Stomach Area} = \text{“Normalized Stomach”}$$

$$\text{Thyroid} - \text{Nose} = \text{“Normalized Thyroid”}$$

Then,

$$\text{Normalized Thyroid}/\text{Normalized Stomach}$$

Mouse No.	ROI analysis	L.S. analysis	Disparity (ROI-LS)
130	0.145	0.089	0.056
131	0.019	0.037	0.018
133	0.080	0.110	0.030
134	0.061	0.041	0.020
135	0.047	0.027	0.020
137	0.089	0.030	0.059

Table X: Comparison of Thyroid Accumulation to Stomach Accumulation one hour after treatment with ¹²⁵I using ROI plots with background subtraction at the nose and standard Liquid Scintillation System.

This method yields good consistency between the two modalities of analysis. We can thus use this more reasonable method of analysis which shows consistency with the liquid scintillation results to search for a relationship between potassium iodide dose and blocking efficacy.

4d. Percent of Injected Dose that the Thyroid Accumulates; Assessment

The next step in the data analysis determined the percentage of radioiodide that accumulates in the thyroid after varying doses of potassium iodide block treatments. To summarize the procedure for analysis:

- (1) Mice were clustered according to the dose of potassium iodide block that they received (no block, 1x, 5x, 10x).
- (2) ROI analysis was performed on each mouse. Counts per ROI for the 55 – 60 time cut are recorded in Table XI in Appendix B. Under the count total, the pixel size of the ROI is recorded.

- (3) The background region was chosen near the nose. This choice is supported by the agreement of the stomach to thyroid ratios between the ROI and liquid scintillation analyses. The nose counts were subtracted on a per pixel basis as described earlier (see Table XI, Appendix B).
- (4) The total body ROI was used as the total injected dose with one distinction. Since the ROI is rectangular, it does not account for the contours of the mouse body. Thus, a per pixel background subtract using an ROI from the detector background away from the mouse was performed (see Table XI, Appendix B).
- (5) Finally, the percentage of the total dose accumulated at the thyroid (and stomach) was determined for each mouse and the results recorded in Table XII.

Dose	File No.	% in Inj. Site	% in Thyroid	% in Stomach
None	69	NA	1.76%	19.0%
None	71	4.39%	2.60%	10.78%
None	73	4.42%	1.82%	14.26%
None	130	0.39%	2.31%	12.81%
1x	133	1.22%	1.85%	17.65%
1x	134	1.50%	1.60%	20.30%
5x	135	6.87%	0.27%	13.23%
5x	137	1.06%	0.77%	10.22%
10x	70	1.33%	0.35%	18.05%
10x	72	8.80%	0.41%	14.21%
10x	74	11.88%	1.14%	6.30%
10x	131	NA	0.77%	14.76%

Table XII: Percentage of total injected dose of ^{125}I in thyroid and stomach after one hour of imaging.

To summarize the results from Table XII, Table XIII gives the average percentage of uptake by the thyroid, the range of values, and the percent error for each group of mice.

Blocking Dose	Mean % uptake by thyroid +/- stand. dev.	Range in values	No. of mice in group
None	2.12% +/- 0.70%	1.76% - 2.60%	4
1x	1.73% +/- 0.18%	1.60% - 1.85%	2
5x	0.52% +/- 0.35%	0.27% - 0.77%	2
10x	0.67% +/- 0.63%	0.35% - 1.14%	4

Table XIII: Mean percent uptake +/- one standard deviation by thyroid for each cohort.

This study involved many steps that could introduce uncertainties. For example, these include preparation of the KI block solution, aliquoting the appropriate amount, the amount of block the animal actually ingested, preparation of the radioisotope dose and its administration. Estimation of the variation at each step, percent errors in the range of 20% – 40% are likely. Considerable overlap is seen in the 5x and 10x groups. This could be because the 5x dose does successfully saturate the thyroid with stable iodide and therefore any additional stable KI does not change the outcome. It is difficult, however, to determine to high accuracy that one is precisely measuring the thyroid's accumulated activity. Large uncertainties can be expected in correlating the raw numbers obtained from liquid scintillation with those from the ROI plots; it would be useful to have an independent assessment of our results in Table XIII. The ratio of thyroid accumulation between each cohort of mice was determined. By dividing each mean in Table XIII by the lowest number, a the relationship of no block to 1x dose to 5x dose to 10x dose was found to be 4.1 to 3.3 to 1 to 1.3, respectively. While we validated the ROI method with the liquid scintillation results, in calculating Table XIII's percent uptake of ^{125}I , only the data obtained via ROI analysis were used. The ability to study in vivo the biodistribution of iodide using a non-invasive protocol has been the goal of the current analysis. To see if the ROI results correlate to the LS data, the ratios of ^{125}I in the thyroid using the LS

data would confirm our analysis method. Normalized thyroid ratios can provide a truly independent assessment of the results. We chose to normalize the raw thyroid counts from LS against the gut. Ideally, we should normalize against a consistent volume of blood. However, the cardiac puncture procedure (the method of retrieving blood from the animal) allows variations in the volume of blood. Thus, the gut was selected because it is easily separated and large. Table XIV shows these results.

Dose	Mouse No.	Thyroid	Gut	Normalized Thyroid	Average for each dose
None	130	67196.09	156557.2	0.429	0.429
1x	133	60962.63	100846.4	0.605	0.405
1x	134	24563.37	120041.0	0.205	
5x	135	13989.03	112293.3	0.125	0.118
5x	137	17840.81	161453.5	0.111	
10x	131	18524.37	122099.5	0.152	0.152

Table XIV: Thyroid counts obtained from liquid scintillation counting normalized with the gut. Averages for each group listed in last column.

The same relationship among the cohorts was found as with the LS data. For no block to 1x dose to 5x dose to 10x dose the relationship was found to be 3.6 to 3.4 to 1 to 1.3, respectively. This indicates reasonable consistency between the two methods of analysis. Therefore, we feel confident that Table XIII displays appropriate comparative uptake by the thyroid one-hour post-exposure to ^{125}I . The data suggest that the blocking is not totally effective for mice at the 1x dose of potassium iodide. At 5x and 10x we reach the saturation point noted in other studies. Yu and Shaw see a plateau at 2 mg KI/kg body mass in rats, which corresponds to our “1x” dose. However, they note further suppression of radioiodide uptake possible with the addition of KClO_4 a known competitor with iodide for NIS transport even at the 1x dose. This suggests that KI at the current recommended dose of 130 mg/70 kg body mass is not the most effective protocol to block the mouse thyroid from uptake of radioiodine. Further evidence that this

blocking dose may not be totally effective in humans is illustrated by the thyroid damage observed in patients undergoing ^{131}I -MIBG treatment. Our current set-up and analysis method will permit us to continue study on other potential methods to protect the thyroid from radioiodine exposure. We believe the ROI method of analysis is reliable because of its good correlation the LS data. Furthermore, it measures the total injected dose and fraction taken up in the thyroid using the same modality and geometry and allows for non-invasive, *in vivo* study. Investigation may be useful to determine a more effective prophylaxis for humans in the event of planned or accidental exposure to radioiodine.

5. Conclusion

The interdisciplinary investigation discussed in this thesis encompassed two aspects. The first portion was a detector development study. Findings of improved spatial resolution with the addition of glass as a method of optical coupling may be applied in future detector design. Specifically, this result can be applied in the set-up of the two new H8500 Hamamatsu PSPMT detectors. The second part of this study focused on the application of the imaging system to physiologic study of small animals. This work suggests that further work may be indicated to determine an optimal means to block uptake of radioiodine by the thyroid.

Appendix A

Table III: Summary of previous studies performed. Time of administration of block and time of analysis are both based on the assumption that the isotope was given at time, t. Times are represented at +/- that reference time. Missing entries in chart are result of information lacking in the reference. ID stands for “injected dose” of radiation; assume uptake at thyroid unless otherwise noted.

Reference	Animal	Isotope and amt.	Amt. of block (mass of iodine)	Time of block	Time of analysis	Result Summary (ID = injected dose)	Notes/Type of analysis used
Hamilton and Soley, 1940	Human, euthyroid	888 – 3700 kBq of radioiodine	14 mg (NaI)	0	+24 hr.	3% ID	These studies combined suggest substantial, but not complete blocking with 14 mg.
Hamilton, 1942	Human, euthyroid	“ “	0.1 µg (NaI)	0	+24 hr.	18.5% ID	
Childs et. al., 1950	Human, euthyroid		0.001 mg	0	+24 hr.	70% ID	This suggests a saturation occurring with a dose of 10 mg. High percentages overall.
			1.0 mg	0	+24 hr.	34.3% ID	
			10 mg	0	+24 hr.	7.6% ID	
			100 mg	0	+24 hr.	5.5% ID	
			380 mg	0	+24 hr.	4.0% ID	
Sternthal et. al., 1980	Human, euthyroid	¹²³ I	0	NA	+24 hr.	19.5% ID	This suggests saturation occurring at 30 mg.
			10 mg	~ 5 min	+24 hr.	12.5% ID	
			30 mg	~ 5 min	+24 hr.	1.5% ID	
			50 mg	~ 5 min	+24 hr.	1.5% ID	
			100 mg	~ 5 min	+24 hr.	0.7% ID	
Pahuja, et. al., 1993	Rat, euthyroid	74 kBq (~2 µCi) ¹³¹ I-NaI	0 mg	NA	+24 hr.	35.1% ID	Study also involved varying time of block; greatest block occurred for time listed. Significant block.
			0.2 mg (~2 mg/kg)	0	+24 hr.	0.4% ID	

Reference	Animal	Isotope and amt.	Amt. of block (mass of iodine)	Time of block	Time of analysis	Result Summary	Notes/Type of analysis used
Zuckier, et. al., 1998	Mouse, euthyroid	0.3 μ Ci 131 I-NaI	0	NA	+24 hr.	11.23% ID	Substantial blocking; specially designed whole-body scintillation counter used (W.B. Johnson&Ass.)
			60 μ g (~2 mg/kg)	- 1 day	+24 hr.	1.73% ID	
Ribela, et. al., 1999	Dog, euthyroid	125 I	25 mg	0	4 – 6 hr.	90% protective effect	Urineanalysis method; optimal dose for dog (25 mg) corrected for weight was nearly as effective in humans.
	Human, euthyroid	125 I	100 mg (~2 mg/kg)	0	4 – 6 hr.	68% protective effect	
Zanzonico and Becker, 2000	Computer modeling of Human, euthyroid	131 I	100 mg (~2 mg/kg)	- 24 hr.	Summed over 3 day period	93% protective effect	Shows substantial blocking based on “compartmental-based” computer modeling of human thyroid metabolism.
				+2 hr.	Summed over 3 day period	80% protective effect	
Yu and Shaw, 2003	Rat, euthyroid	148 kBq of 131 I (~4 μ Ci)	0	NA	+24 hr.	9.9% ID	“cuff method” described earlier; saturation effect is seen at 2 mg/kg of body weight.
			1 mg/kg	-2 hr.	+24 hr.	4.0% ID	
			2 mg/kg	-2 hr.	+24 hr.	2.8% ID	
			4mg/kg	-2 hr.	+24 hr.	2.7% ID	
Zuckier, et. al., 2004	Mice, euthyroid	63 kBq of 123 I-NaI (~2 μ Ci)	0	NA	+1 hr.	5-7% uptake at thyroid; 20-25% at stomach; ~2% mediastinal	Study did not look at effect of KI blocking, but used ROI analysis to determine distribution of iodide in the body.

Appendix B

Table XI: ROI analysis to determine percent uptake by the thyroid. Noted in parenthesis under counts listed is pixel size of ROI. The second column under each area of interest is the counts per ROI with the background subtracted out.

Dose	File No.	Total Body		Detector Noise	Injection Site		Thyroid		Stomach		Nose
None	69	973.202 (75x23)	722.15	14.5540 (10x10)	20.2938 (7x7)	NA	24.1001 (4x4)	12.72	176.853 (7x8)	137.03	11.3787 (4x4)
None	71	1444.89 (25x80)	1106.27	16.9308 (10x10)	98.2595 (7x10)	48.58	40.1322 (4x4)	28.78	154.024 (7x7)	119.25	11.3545 (4x4)
None	73	1594.39 (25x80)	1379.61	10.7392 (10x10)	91.6808 (8x8)	61.03	32.7448 (4x4)	25.08	219.750 (8x6)	196.76	7.66270 (4x4)
None	130	5892.62 (18x75)	5545.86	25.6859 (10x10)	278.442 (7x12)	21.49	176.830 (4x4)	127.88	881.696 (8x7)	710.39	48.9479 (4x4)
1x	133	6269.15 (20x78)	5790.23	30.7005 (10x10)	262.132 (8x8)	70.39	154.826 (4x4)	106.90	1165.96 (8x6)	1022.15	47.9300 (4x4)
1x	134	6224.69 (20x77)	5922.44	19.6268 (10x10)	316.038 (8x10)	88.99	140.355 (4x4)	94.95	1384.34 (8x8)	1202.70	45.4096 (4x4)
5x	135	5642.00 (20x78)	5233.67	26.1749 (10x10)	681.275 (10x10)	359.69	65.3655 (4x4)	13.91	898.005 (8x8)	692.19	51.4544 (4x4)
5x	137	6290.20 (18x78)	6055.44	16.7207 (10x10)	298.738 (8x8)	64.40	105.028 (4x4)	46.44	984.852 (10x10)	618.70	58.5834 (4x4)
10x	70	950.711 (75x23)	843.61	6.20865 (10x10)	30.5499 (8x8)	11.20	7.80368 (4x4)	2.97	166.811 (6x8)	152.30	4.83740 (4x4)
10x	72	1706.96 (25x85)	1490.93	10.1660 (4x4)	186.444 (10x10)	131.16	14.8821 (4x4)	6.04	238.450 (6x8)	211.92	8.84449 (4x4)
10x	74	1520.74 (25x80)	1315.51	10.2616 (10x10)	183.325 (5x10)	156.27	23.6769 (4x4)	15.02	108.812 (8x6)	82.84	8.65862 (4x4)
10x	131	6053.18 (20x77)	5682.83	24.0489 (10x10)	222.210 (9x10)	NA	86.8589 (4x4)	43.60	1011.77 (8x8)	838.75	43.2551 (4x4)

Appendix C: Computer Proficiency Requirement

The following is a computer program written in the CSL of the data acquisition software to extract a certain region of a histogram. Thus, SPECT reconstruction can occur with just that portion of the histogram; not the whole image.

```
.*****
;
;KILLREGION
;
;
;WRITTEN BY JULIE CELLA
;
;
;THIS IS A K_MAX PROGRAM THAT WILL
;KILL CERTAIN REGIONS UNNESSARY TO
;THE SPECT RECONSTRUCTION
;
;
;PRECONDITION:
; HISTOGRAMS RECORDED AT EACH DEGREE ARE
; SAVED AS:
; "XXXXXXXXX #1"
; WHERE XXXXXXXXXX IS THE NAME OF THE FILE
; #1 IS THE INDEXING NUMBER REFERING TO ANGLE
; AT WHICH IMAGE WAS RECORDED
;
;
;POSTCONDITION:
; NEW FILES ARE WRITTEN WITH THE UNWANTED
; AREAS ELIMINATED. THE OLD FILES ARE
; NOT CHANGED.
.*****
;
.*****
;
;DECLERATION OF VARIABLES AND EVENTS
.*****
;
DECLARE KILLREGION AS EVENT; CALLED IN C40
DECLARE C2 AS EVENT ; LEFT LIMIT
DECLARE C4 AS EVENT ; RIGHT LIMIT
DECLARE C6 AS EVENT ;TOP LIMIT
DECLARE C8 AS EVENT ; BOTTOM LIMIT
DECLARE C10 AS EVENT ;FIRST NUMBER
DECLARE C20 AS EVENT ;ANGLE INCREMENT
DECLARE C30 AS EVENT ; SECOND NUMBER
DECLARE C40 AS EVENT ;CALLS KILLREGION

;THE NAME OF THE FILE TO BE WRITTEN
DECLARE FILENAME_W AS STRING
;THE NAME OF THE FILE TO BE READ
DECLARE FILENAME_R AS STRING
```

```

DECLARE WL AS INTEGER
DECLARE WR AS INTEGER
DECLARE WB AS INTEGER
DECLARE WT AS INTEGER

;AN INDEXING NUMBER
DECLARE NUMBER AS INTEGER
;THE ANGLE INCREMENT OF NEXT HISTOGRAM
DECLARE DELTA AS INTEGER
;THE FIRST ANGLE
DECLARE FIRST_NUMBER AS INTEGER
;THE LAST ANGLE
DECLARE LAST_NUMBER AS INTEGER
;A PLACE HOLDER FOR THE CREATION OF SUFFIX
DECLARE SUFFIX AS STRING
DECLARE MYTEXT AS STRING
DECLARE NUMBER2 AS INTEGER
; FOR READING THE PIXELS OVER TO THE NEW IMAGE
DECLARE XCHAN AS INTEGER
DECLARE YCHAN AS INTEGER

; FOR SPECIFYING THE REGION TO "KILL"
DECLARE XRANGE AS INTEGER
DECLARE YRANGE AS INTEGER

.*****
;
;MAIN CODE
.*****
;

ON GO DO

END

ON KILLREGION DO
  RECORDLN " _____ "
  SET TEXT TO FIRST_NUMBER

  PROMPT WITH "PLEASE ENTER START NUMBER"
  IF (OK) THEN
    SET FIRST_NUMBER TO TEXT
  END IF

  PROMPT WITH "PLEASE ENTER FINISH NUMBER"
  IF (OK) THEN

```

```

    SET LAST_NUMBER TO TEXT
END IF

PROMPT WITH "PLEASE ENTER DELTA"
IF (OK) THEN
    SET DELTA TO TEXT
END IF
SET NUMBER TO FIRST_NUMBER

REPEAT
,*****INSERT FILE NAMES BELOW*****
SET FILENAME_R TO "spect_C_A"
SET FILENAME_W TO "spect_C_A_fixed"
,*****
CONCAT_STR FILENAME_W " "
CONCAT_STR FILENAME_R " "
SET SUFFIX TO NUMBER
CONCAT_STR FILENAME_W SUFFIX
CONCAT_STR FILENAME_R SUFFIX
NUMBER2 = NUMBER + DELTA

;OPENING THE READ FILE; GETTING INFO
OPEN FILENAME_R
GET CURSORS IN WL WR WB WT
;MAKING NEW HISTOGRAM FOR WRITE DATA
NEW HISTOGRAM FILENAME_W 128 128
SET AXES TO FALSE
SET CURSORS TO WL WR WB WT

;THIS CODE WILL TRANSFER THE DATA OVER TO THE NEW FILE
FOR XCHAN = 0 TO 127
    FOR YCHAN = 0 TO 127
        {FILENAME_W}[XCHAN, YCHAN] = {FILENAME_R}[XCHAN, YCHAN]
    END FOR
END FOR
CLOSE FILENAME_R

SET TEXT TO LEFT_LIMIT
SET MYTEXT TO "left limit/"
CONCAT_STR MYTEXT TEXT
SET_CONTROL 2, 0, MYTEXT

SET TEXT TO RIGHT_LIMIT
SET MYTEXT TO "right limit/"

```

```
CONCAT_STR MYTEXT TEXT
SET_CONTROL 4, 0, MYTEXT
```

```
SET TEXT TO TOP_LIMIT
SET MYTEXT TO "top limit/"
CONCAT_STR MYTEXT TEXT
SET_CONTROL 6, 0, MYTEXT
```

```
SET TEXT TO BOTTOM_LIMIT
SET MYTEXT TO "bottom limit/"
CONCAT_STR MYTEXT TEXT
SET_CONTROL 8, 0, MYTEXT
```

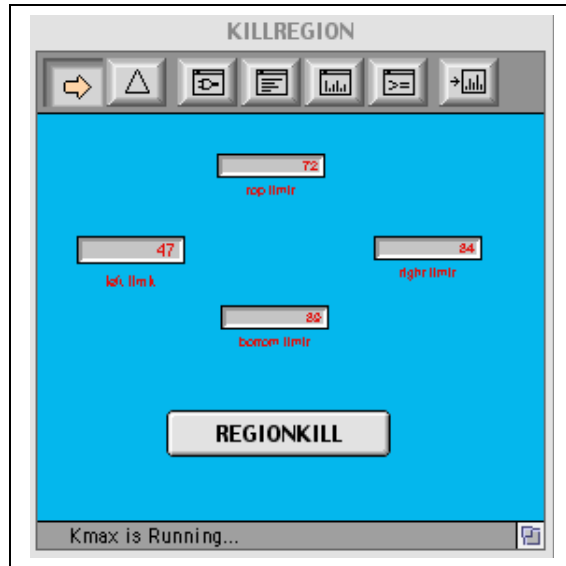
```
;THIS CODE WILL DELETE COUNTS IN UNWANTED REGION
FOR XRANGE = 0 TO LEFT_LIMIT
  FOR YRANGE = 0 TO 127
    {FILENAME_W}[XRANGE, YRANGE] = 0
  END FOR
END FOR
```

```
FOR XRANGE = LEFT_LIMIT TO RIGHT_LIMIT
  FOR YRANGE = TOP_LIMIT TO 127
    {FILENAME_W}[XRANGE, YRANGE] = 0
  END FOR
END FOR
```

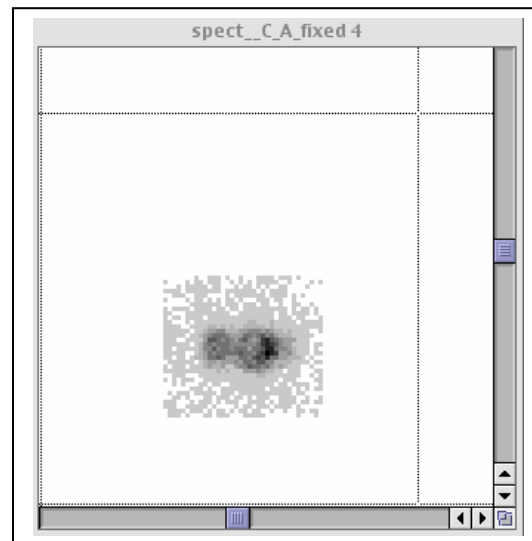
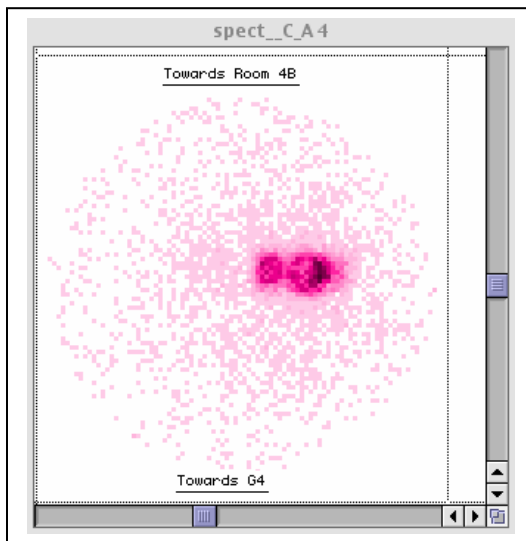
```
FOR XRANGE = RIGHT_LIMIT TO 127
  FOR YRANGE = 0 TO 127
    {FILENAME_W}[XRANGE, YRANGE] = 0
  END FOR
END FOR
```

```
FOR XRANGE = LEFT_LIMIT TO RIGHT_LIMIT
  FOR YRANGE = 0 TO BOTTOM_LIMIT
    {FILENAME_W}[XRANGE, YRANGE] = 0
  END FOR
END FOR
```

```
SAVE FILENAME_W
CLOSE FILENAME_W
RECORDLN "new histogram complete and saved"
NUMBER = NUMBER + DELTA
UNTIL (NUMBER>LAST_NUMBER-DELTA)
END
Interface of Instrument Created:
```



“Before” and “After” Histograms:



References

1. Balk SJ, Miller RW, Shannon MW. Radiation disasters and children. *Pediatrics*. 2003; 111: 1455-1467.
2. Brans B, Monsieurs M, Laureys G, Kaufman JM, Thierens H, Dierckx RA. Thyroidal uptake and radiation dose after repetitive I-131-MIBG treatments: influence of potassium iodide for thyroid blocking. *Med Pediatr Oncol*. 2002; 38: 41-46.
3. van Santen HM, de Kraker J, van Eck BLF, de Vijlder JJM, Vulsma T. High incidence of thyroid dysfunction despite prophylaxis with potassium iodide during I-131-metaiodobenzylguanidine treatment in children with neuroblastoma. *Cancer*. 2002; 94: 2081-2089.
4. Castronovo FP Jr. I-125-fibrinogen: thyroid blocking with 2.5 mg potassium iodide twice daily in patients after hip surgery. *J Nucl Biol Med*. 1994; 38: 55-60.
5. Jacob P, Kenigsberg Y, Goulko G, Buglova E, Gering F, Golovneva A, Kruk J, Demidchik EP. Thyroid cancer risk in Belarus after comparison with external exposures. *Radiat Environ Biophys*. 2000; 39: 25-31.
6. Gilbert ES, Tarone R, Bouville A, Ron E. Thyroid cancer rates and I-131 doses from Nevada atmospheric nuclear bomb tests. *Journal of the National Cancer Institute*. 1998; 90: 1654-1660.
7. US Food and Drug Administration, Center for Drug Evaluation and Research. Guidance Document: Potassium Iodide as a Thyroid Blocking Agent in Radiation Emergencies. Available at: <http://www.fda.gov/cder/guidance/4825fnl.htm>. Accessed January 30, 2004.
8. Zuckier LS, Dohan O, Li Y, Chang CJ, Carrasco N, Dadachova E. Kinetics of Perrhenate Uptake and Comparative Biodistribution of Perrhenate, Pertechnetate, and Iodide by NaI Symporter-Expressing Tissues In Vivo. *The Journal of Nuclear Medicine*. 2004; 45: 500-507.
9. Dingli D, Russell SJ, Morris JC III. In vivo imaging and tumor therapy with the sodium iodide symporter. *Journal of Cellular Biochemistry*. 2003; 90: 1079-1086.
10. He J, Liu G, Zhang S, Rusckowski M, Hnatowich D. Pharmacokinetics in mice of four oligomerconjugated polymers for amplification targeting. *Cancer and Biotherapy and Radiopharmaceuticals*. 2003; 18: 941-947.

11. Pahuja DN, Rajan MGR, Borkar AV, Samuel AM. Potassium Iodate and its comparison to Potassium Iodide as a blocker of ¹³¹I uptake by the thyroid in rats. *Health Physics*. 1993; 65: 545-549.
12. Zuckier LS, Li Y, Chang CJ. Evaluation in a mouse model of a thyroid-blocking protocol for ¹³¹I antibody therapy (Short Communication). *Cancer Biotherapy and Radiopharmaceuticals*. 1998; 13: 457-460.
13. Ribela MT, Marone MM, Bartolini P. Use of radioiodine urinalysis for effective thyroid blocking in the first few hours post exposure. *Health Physics*. 1999; 76: 11-16.
14. Takamura N, Hamada A, Yamaguchi N, Matsushita N, Tarasiuk I, Ohashi T, Aoyagi K, Mine M, Yamashita S. Urinary iodine kinetics after oral loading of potassium iodine. *Endocrine Journal*. 2003; 50: 589-593.
15. Yu MD, Shaw SM. Potential interference of agents on radioiodide thyroid uptake in the euthyroid rat. *The Journal of Nuclear Medicine*. 2003; 44: 832-838.
16. Zanzonico PB, Becker DV. Effects of time of administration and dietary iodine levels on potassium iodide (KI) blockade of thyroid irradiation by ¹³¹I from radioactive fallout. *Health Physics*. 2000; 78: 660-667.
17. Chu T, Li R, Hu S, Liu X, Wang X. Preparation and biodistribution of technetium-99m-labeled 1-(2-nitroimidazole-1-yl)-propanhydroxyiminoamide (N21PA) as a tumor hypoxia marker. *Nuclear Medicine and Biology*. 2004; 31: 199-203.
18. Childs DS, Keating FR, Rall JE, Williams MMD, Power MH. The effect of varying quantities of inorganic iodide (carrier) on the urinary excretion and thyroidal accumulation of radioiodine in exophthalmic goiter. *J Clin Invest*. 1950; 29: 726-738.
19. Sternthal E, Lipworth L, Stanley B, et al. Suppression of thyroid radioiodine uptake by various doses of stable iodide. *New England Journal of Medicine*. 1980; 19: 1083-1088.

Bibliography

Bacher K, Brans B, Monsieurs M, De Winter F, Dierckx RA, Thierens H. Thyroid uptake and radiation dose after ^{131}I -lipiodol treatment: is thyroid blocking by potassium iodide necessary? *European Journal of Nuclear Medical Molecular Imaging*. 2002; 29: 1311-1316.

Becker DV, Braverman LE, Dunn JT, Gaitan E, Gorman C, Maxon H, Schneider AB, Van Middlesworth L, Wolff J. The use of iodine as a thyroidal blocking agent in the event of a reactor accident. Report of the Environmental Hazards Committee of the American Thyroid Association. *Journal of the American Medical Association*. 1984; 252: 659-661.

